MICROPOROUS AND MESOPOROUS MATERIALS

ZEOLITES, CLAYS, CARBONS AND RELATED MATERIALS

On-line Access via: www.elsevier.com/locate/micromeso

Removal of lead ions by fixed bed of clinoptilolite – The effect of flow rate

N. Vukojević Medvidović, J. Perić, M. Trgo *, M.N. Mužek

University of Split, Faculty of Chemistry and Technology, Teslina 10/V, 21000 Split, Croatia

Abstract

The removal of lead ions from aqueous solutions by means of a fixed bed of natural zeolite clinoptilolite has been investigated. Isothermal column experiments were performed under a constant inlet concentration and bed depth, and different flow rates. The capacities of the breakthrough and exhaustion points do not change significantly with the increase of the flow rate, while the time needed to reach breakthrough is significantly shorter. To determine the kinetic constants, the equation by Yoon and Nelson was applied to the experimental results. The rate proportionality constant K_{YN} increases and the time τ decreases with the increase of the lead solution flow. Based on these parameters the modelled breakthrough curves have been obtained, and they are in agreement with the corresponding experimental data. The parameters of the Yoon–Nelson model have been successfully used for scaling up the bed depth of the examined system, and a satisfactory agreement of experimental and predicted breakthrough curves has been obtained.
© 2007 Elsevier Inc. All rights reserved.

1. Introduction

The presence of heavy metals in the environment can be detrimental to all living organisms including humans. This pollution originates from discharge effluents from industries such as cement industries, electro plating, production of metal alloys, production of pigments for paints, mining, etc. Different treatments have been used in removal of heavy metals particularly from wastewaters; and adsorption/ion exchange using natural materials has yielded high-quality treated water at satisfactory costs. One of commonly used natural adsorbents and ion exchangers is natural zeolite clinoptilolite, which is suitable for removal of heavy metals from waters and wastewaters down to very low concentrations. Clinoptilolite as a natural zeolite is an alumosilicate mineral with a specific structure consisting of a two-dimensional system of three types of channels. They are occupied by hydrated exchangeable ions responsible for its ion exchange and molecular sieve properties [1,2]. The process of removal of lead ions from aqueous solutions on clinoptilolite is usually performed by the batch method or by the column method [3–7]. The batch method is easily performed in a laboratory study, but is less convenient for industrial application. The fixed bed columns are widely used in chemical industry because of the simplicity of their application and the possibility of regeneration of ion exchangers. The efficiency of the column performance depends on dimensions of the column, particle size and depth of the bed of clinoptilolite, and the flow rate and concentration of the aqueous solution of lead ions [7–11]. The aim of this paper is to optimise the flow of the influent solution by means of the time needed for breakthrough and exhaustion, and by means of the capacity of the fixed bed of zeolite.

2. Material and methods

The natural zeolite sample originated from the Vranjska Banja deposit (Serbia). The sample was crushed up and sieved to the particle size fraction 0.6–0.8 mm, rinsed in

---

* Corresponding author. Tel.: +385 21 329 454; fax: +385 21 329 461.
E-mail address: mtrgo@ktf-split.hr (M. Trgo).

doubly distilled water in order to remove possible impurities that might induce clogging during the process in the column. After drying at 60°C, the samples were stored in the dessicator.

The chemical composition of the zeolite sample was determined by the classical chemical analysis of alumosilicates [12], and was, in mass%, SiO_2 – 66.36; Al_2O_3 –13.81; Fe_2O_3 – 1.69; MgO – 1.03; CaO – 3.65; K_2O – 0.99; Na_2O – 1.03; loss of ignition – 13.40. The X-ray diffraction method was used for qualitative mineralogical analysis, on a "Philips-CubiX XRD" diffractometer (CuKα radiation, $2\theta = 0$–60, 0.03 2θ/s). The mineralogical analysis has shown the major zeolite mineralogical component to be clinoptilolite whose part in the sample was ≈80%.

A solution of lead ions with the concentration of 1.024 mmol/l was prepared by dissolving $Pb(NO)_3$ in doubly distilled water. Experiments were carried out in a glass column with the inner diameter of 12 mm and a height of 500 cm, filled with 2.9 g (4.5 cm³) of the clinoptilolite sample to the bed depth of 40 mm. Isothermal experiments at 20°C were performed at the constant inlet concentration and bed depth with changes of flow rates through the fixed bed of 1, 2 and 3 ml/min. The solution flowed from the top of the column (the down flow mode), and passed through the fixed zeolite bed, the flow constancy being maintained by a vacuum pump. At selected time intervals the lead concentration was determined in the effluent by the complexometric method in the acid medium, using a highly selective indicator, methylthymolblue [13]. The process was stopped when the Pb concentration in the effluent reached the initial concentration in the influent. After each service cycle of the exchange, a regeneration cycle took place with the solution of sodium nitrate with the concentration of $NaNO_3$ of 176.5 mmol/l (15 g/l), by passing the solution from the top of the column through the fixed zeolite bed. The regeneration process was stopped when the Pb concentration in the effluent became constant. Each service cycle as well as the regeneration cycle was repeated and the plots present the mean values. During the process, the changes of the pH value were measured in the influent and in the effluent.

Scanning electron microscopy and energy dispersive X-ray (SEM-EDX) analyses of natural zeolite, zeolite after the service cycle at a flow rate of 1 ml/min and initial concentration of 1.024 mmol/l, and after the regeneration cycle were performed using Zeiss DSM 962 and INCA Energy Dispersive Microanalysis. The qualitative EDX analysis was performed on the all area of the SEM image, based on the K_α lines of radiation for each element examined.

3. Results and discussion

The curves show the experimental results for the column method, as the ratio of outlet and initial concentrations versus the bed volume (BV) (Fig. 1).

The curves in Fig. 1 are characterized by breakthrough and exhaustion points, and corresponding capacities. The capacity in the breakthrough point C_B is defined as the
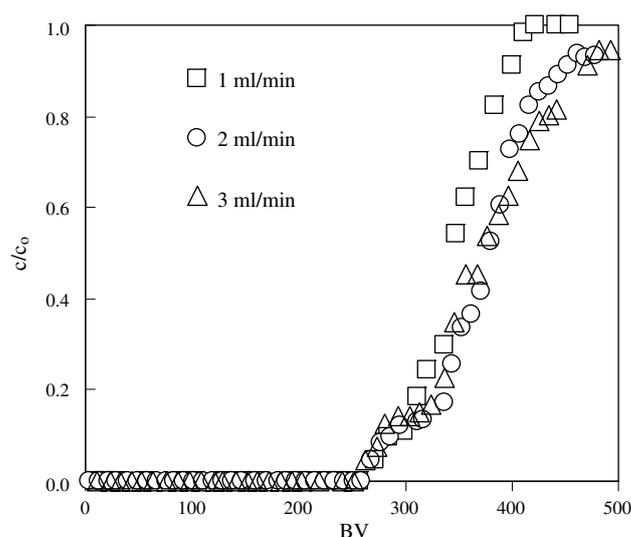

Fig. 1. Breakthrough curves for lead removal for different flows expressed as c/c_o versus BV (ratio of the solution volume and the fixed bed volume).

amount of lead ions bound on zeolite when the concentration of lead in the effluent reaches ≈5% of the initial concentration [8]:

$$C_B = \frac{\int_0^{V_B}(c_o - c)\mathrm{d}V}{\rho H A} = \frac{n_B}{m} = \frac{c_o V_B}{m} \tag{1}$$

where

C_B	capacity at the breakthrough point (mmol/g)
c_o	influent concentration (mmol/l)
c	effluent concentration (mmol/l)
V_B	volume of solution passed in the breakthrough point (ml)
ρ	packing density of the bed (g/cm³)
H	bed depth (cm)
A	bed cross-sectional area (cm²)
n_B	amount of lead removed up to breakthrough point (mmol)
m	mass of the bed (g)

The capacity in the exhaustion point C_E corresponds to the amount of lead ions bound on zeolite when the concentration of lead in the effluent reaches ≈95% of the initial value:

$$C_E = \frac{\int_0^{V_E}(c_o - c)\mathrm{d}V}{\rho H A} = \frac{n_E}{m} \tag{2}$$

where

C_E	capacity at the exhaustion point (mmol/g)
n_E	amount of lead removed up to exhaustion point (mmol)
V_E	volume of solution passed up to the exhaustion point (ml)

According to Michaels, during the process, the feed solution containing lead ions passes through the fixed bed

of zeolite, and a mass transfer zone forms in which the fresh solution is in contact with unsaturated zeolite [14]. This zone also moves through the column and reaches exit in the exhaustion point. The height of the mass transfer zone h_Z is defined as [8,10]:

$$h_Z = H(V_E - V_B)/[V_E - (1 - F) \cdot (V_E - V_B)], \qquad (3)$$

where F – parameter measuring the symmetry of the breakthrough curve, or the fraction of zeolite present in the bed that still possesses the ability to remove ions.

The parameter F can be calculated from the equation:

$$F = \frac{n_Z}{n_E} = \frac{\int_{V_B}^{V_E}(c_o - c)dV}{c_o(V_E - V_B)}$$
$$= \int_0^1 \left(1 - \frac{c}{c_o}\right)d\left(\frac{V - V_B}{V_E - V_B}\right) \qquad (4)$$

where

n_Z amount of lead removed between the breakthrough and exhaustion points (mmol)

V effluent volume (ml)

For symmetry of the S-curves, parameter $F \cong 0.5$, Eq. (3) becomes:

$$h_Z = 2 \cdot H \cdot \left[\frac{V_E - V_B}{V_E + V_B}\right]. \qquad (5)$$

The degree of saturation or column efficiency η can be calculated as:

$$\eta = C_B/C_E. \qquad (6)$$

The empty bed contact time, EBCT, or the residence time is usually defined as the relation between the depth of the zeolite bed in the column and the feed solution velocity:

$$EBCT = H/v, \qquad (7)$$

where v is the linear flow rate through the column in $m^3\,m^{-2}\,h^{-1}$.

Fig. 1 clearly shows that, for all flow rates of the solution through the fixed bed, the breakthrough points appear at very close values of BV, i.e., volumes of treated solution. This means that the breakthrough capacities for flow rates examined also have similar values. The time needed for reaching the breakthrough point decreases with higher values of the flow, which is shown in Fig. 2. At higher flow rates, the same volume of the lead ions solution can be treated in a significantly shorter time.

The parameters given by Eqs. (1)–(7) are calculated from the breakthrough curves (Table 1) and represent the main parameters for scaling up the process. At higher flow rate values, the efficiency of the fixed bed negligibly decreases, the empty bed contact time (EBCT) decreases, while the height of the mass transfer zone h_Z increases.

The results calculated in Table 1 show that breakthrough capacities slightly decrease with flow rates, which is a main factor for practical application of this process. This can be
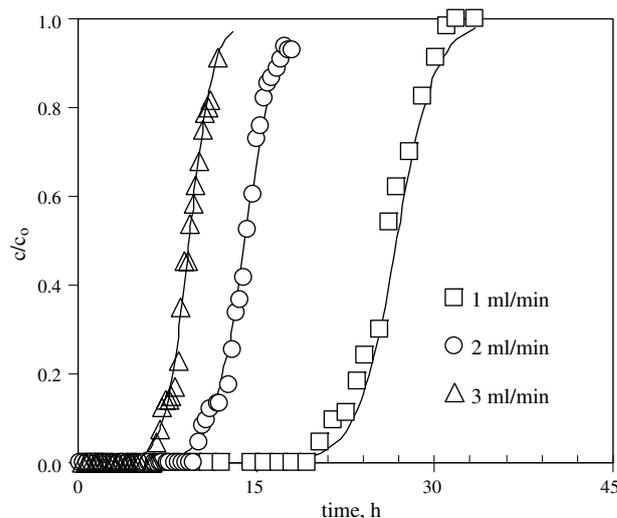

Fig. 2. Breakthrough curves expressed as c/c_o versus time. Fitting of experimental curves (points) to curves obtained from the Yoon and Nelson model (lines).

attributed to the optimal choice of experimental conditions such as the ratio of particle/column diameters, and the ratio of bed depth/column diameter. The exhaustion capacities decrease with the increase of the flow from 1 ml/min to 2 ml/min, and remain constant with the increase of the flow from 2 ml/min to 3 ml/min. The parameter F indicates the symmetry of S-curves, so that, in order to provide an adequate test of suitability of the MTZ model for process description, the height of the mass transfer zone h_Z estimated from Eq. (3) should be equal to the value h_Z' calculated from the following equation ($F = 0.5$) [14]:

$$h_Z' = \frac{n_Z}{(1 - F)C_E\rho A}. \qquad (8)$$

The column efficiency η calculated by Eq. (6) should be equal to the value:

$$\eta' = \frac{H - (1 - F)h_Z'}{H}, \qquad (9)$$

and the capacity at the exhaustion point C_E calculated by Eq. (2) should be equal to the value:

$$C_E' = \frac{C_B H}{H - (1 - F)h_Z'}. \qquad (10)$$

The results of h_Z', η' and C_E' calculated according to Eqs. (8)–(10) show excellent agreement with the values h_Z, η and C_E calculated according to Eqs. (3), (2) and (6) (Table 2), for all examined flow rates. This confirms the symmetry of the breakthrough curves and applicability of the Mass Transfer Zone model in the examined range of flow rates.

The regeneration process refreshes the zeolite for the next service cycle. Fig. 3 shows the regeneration curves obtained during regeneration after each service cycle.

All curves in Fig. 3 show a rapid increase of lead ions concentration in the effluent, followed by a rapid decrease, until the concentration of lead in the regenerate reaches

Table 1
Parameters calculated from the breakthrough curves

Q		Breakthrough point		C_B (mmol/g)	C_E (mmol/g)	η (–)	F (–)	h_Z (cm)	EBCT (min)
ml/min	BV/h	BV	t, h						
1.0	13.3	270.9	20.42	0.433	0.554	0.78	0.50	1.75	4.52
2.0	26.5	268.7	10.04	0.430	0.597	0.72	0.55	2.06	2.26
3.0	39.8	262.1	6.58	0.419	0.594	0.71	0.47	2.42	1.51

Table 2
Comparison of the experimental and corrected results for the parameters h_Z, η and C_E

Q		n_B (mmol)	n_E (mmol)	n_Z (mmol)	h_Z (cm)	h'_Z (cm)	η (–)	η' (–)	C_E (mmol/g)	C'_E (mmol/g)
ml/min	BV/h									
1.0	13.3	1.256	1.607	0.351	1.75	1.75	0.78	0.78	0.554	0.554
2.0	26.5	1.247	1.731	0.484	2.06	2.26	0.72	0.72	0.597	0.599
3.0	39.8	1.215	1.728	0.508	2.42	2.36	0.71	0.71	0.594	0.594

$\approx$0.1 mmol Pb/l. Only 60–65 bed volumes of the regeneration solution were necessary for complete regeneration, which is about 22% of the volume of the feed solution passed in the service cycle. During regeneration, the concentration of lead in the regenerate becomes extremely high and attains values up to approx. 30 mmol/l ($\approx$6 g/l), which makes it possible to reuse the lead ions solution in the process. The percentage of regeneration, α_R, is the ratio of the total amount of lead recovered by the regeneration cycle, n_R, and the amount of lead removed during each service cycle, n_E, up to the exhaustion point:

$$\alpha_R = \frac{n_R}{n_E} \cdot 100. \tag{11}$$

For flow rates of 1, 2 and 3 ml/min, the percentage of regeneration equals 81.1%, 99.8% and 98.3% respectively, which means that for flow rates of 2 and 3 ml/min almost all of lead ions were bound, were recovered. A concentration of lead ions remaining in the regenerate ($<$0.1 mmol/
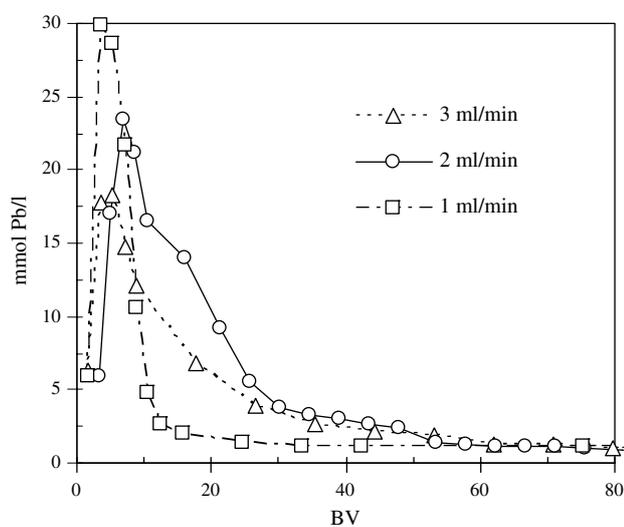

Fig. 3. The change of concentration of lead ions in the effluent during regeneration performed after each service cycle.

l) indicates incompleteness of regeneration. This can be explained by high-affinity of clinoptilolite for lead ions that have small hydrated ionic radii [15,16]. It has been confirmed by the EDX analysis performed on the SEM image of natural zeolite before the experiment (Fig. 4a), a sample after the service cycle with the flow rate of 1 ml/min (Fig. 4b), and the same sample after regeneration with 15 g/l $NaNO_3$ (Fig. 4c).

Fig. 4b shows that a large quantity of lead is bound on natural clinoptilolite, while some quantity of lead remains in the sample after regeneration (Fig. 4c).

Continuous measuring of pH values during service and regeneration cycles has shown that the breakthrough point in the service cycle and the completeness of regeneration can be indicated by a change in pH values. Fig. 5 shows changes of pH values during service and regeneration.

The pH value does not change significantly until the breakthrough point in Fig. 5a, when it decreases by two units. During regeneration, a rapid increase of concentration of lead ions is followed by a decrease in pH values (Fig. 5b), and when concentration of lead in the regeneration effluent is the lowest, pH is the highest. This significant effect is observed in all service and regeneration cycles, and can be used for indication of the breakthrough point and the end of regeneration in practical applications of lead removal on fixed bed columns. The changes of pH values can be explained by the hydrolysis of Pb^{2+} in aqueous solutions according to reaction [15]:

$$Pb^{2+} + H_2O \leftrightarrow Pb(OH)^+ + H^+. \tag{12}$$
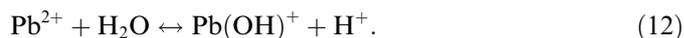
This equation clearly shows that increased concentrations of lead ions favour hydrolysis and reduce the pH in the solution.

It is too difficult to describe the dynamic behaviour of heavy metal removal in a fixed zeolite bed under defined operating conditions because the process does not take place at a steady state while the feed solution passes through the bed. Various simple mathematical models have been developed to describe and possibly predict the
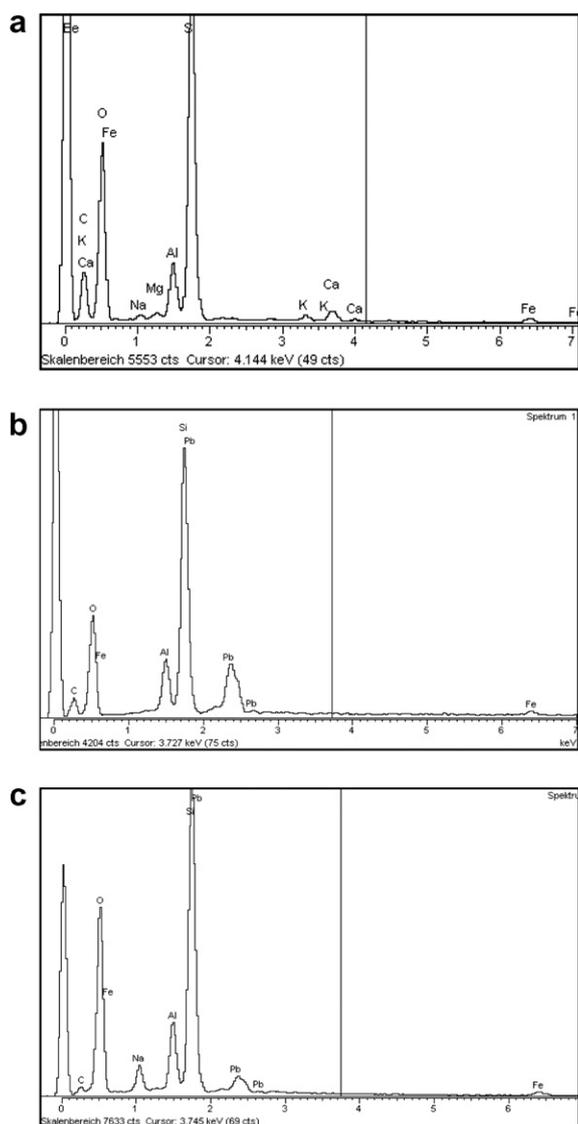
Fig. 4. EDX analysis of (a) natural zeolite, (b) zeolite after service cycle, (c) zeolite after regeneration.

dynamic behaviour of the bed in column performance [17,18]. One of empirical models used for the column method is the model by Yoon and Nelson [19–22]. This model is not only less complicated, but also requires no detailed data about the characteristics of the adsorbate of interest, the type of adsorbent or physical properties of the adsorption bed. Also, this model was not used in literature for results of experiments with zeolite as ion exchanger or adsorbent [23]. The Yoon and Nelson model for a single component system is expressed by Eq. [19]:

$$\ln[c/(c_o - c)] = K_{YN}(t - \tau), \tag{13}$$

K_{YN} proportionality constant (min^{-1})
t time (min)
τ breakthrough time when c/c_o equals 0.5.

Eq. (13) can be rewritten as follows [19–25]:

$$t = \tau + \frac{1}{K_{YN}} \ln\left(\frac{c}{c_o - c}\right). \tag{14}$$

From experimental data for c, c_o, and t at different solution flow rates, graphical dependences have been plotted in Fig. 6.

The linear dependence of $\ln[c/(c_o - c)]$ versus time, for all flow rates examined, indicates a satisfactory fitting of experimental points to the model, and from these lines the parameters of the model (K_{YN} and τ) have been calculated and presented in Table 3.

For a symmetrical shape of the breakthrough curve, the zeolite bed should be completely saturated at 2τ, when the amount of lead bound in the zeolite is half that of the total lead entering the zeolite bed within the 2τ period, and corresponds to the total capacity C_τ [21]:

$$C_\tau = \frac{c_o Q \tau}{m}. \tag{15}$$

In order to provide an adequate test of the Yoon–Nelson model equation, the total capacity C_E calculated from the
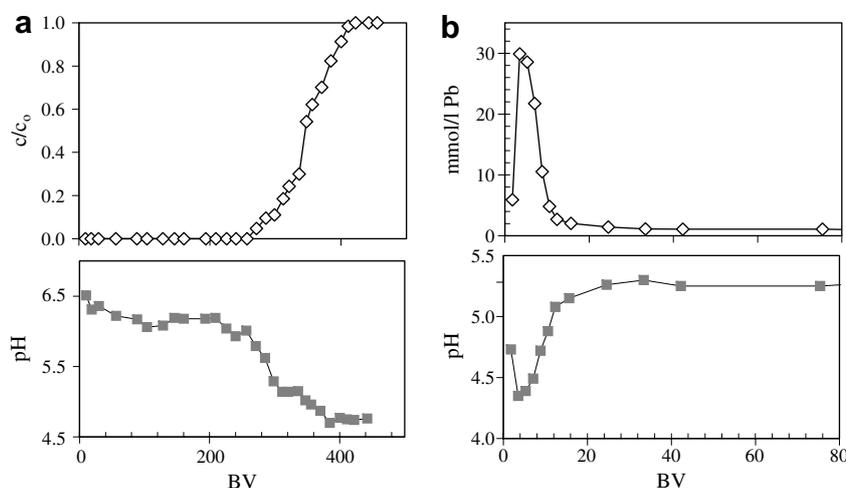

Fig. 5. Changes of the pH value during (a) the service cycle, (b) the regeneration cycle.
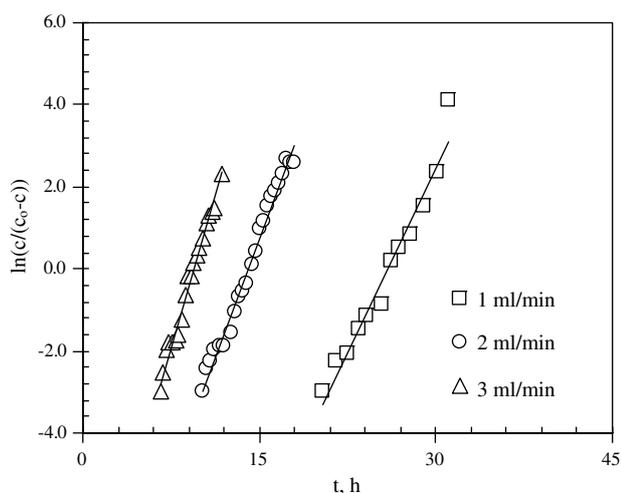
Fig. 6. Testing of experimental results by the Yoon–Nelson equation.

Table 3
The parameters calculated from the tested Yoon–Nelson model

Q (ml/min)	k_{YN} (h^{-1})	τ (h)	τ_{exp} (h)	R^2	C_τ (mmol/g)	C_E (mmol/g)
1.0	0.603	26.83	26.17	0.954	0.570	0.554
2.0	0.756	14.08	14.17	0.983	0.597	0.597
3.0	1.000	9.40	9.33	0.983	0.599	0.594

area above the S-curves up to the saturation point should be equal to the value determined from Eq. (15), and the results are compared in Table 3. Also, Table 3 compares values of τ calculated from the model with τ_{exp} determined from the experimentally obtained breakthrough curves. The agreement of experimentally obtained and calculated parameters in Table 3 confirms the applicability of the Yoon–Nelson equation to the system examined. Insertion of calculated parameters K_{YN} and τ into Eq. (13) for randomly chosen values of time t yields modelled breakthrough curves that are shown by lines in Fig. 2. Excellent fitting of the experimental and modelled breakthrough curves additionally confirms that mass transport through a fixed bed of zeolite follows the assumptions of the Yoon–Nelson model. Namely, the proportionality constant K_{YN} slightly increases with the flow rate which means that the mass transport resistance decreases. The value of τ decreases, due to faster saturation of the fixed bed with the increased flow rate of the feed solution. The mass transport resistance is proportional to axial dispersion and thickness of the liquid film on the particle surface. In our case the flow rates are small enough and their effect on the increase of axial dispersion is negligible, which is confirmed by the increase of the proportionality constant. Therefore, we assume that the increase of the flow rate increases the driving force of mass transfer in the liquid film. A similar dependence of the proportionality constant on the flow rate has been observed in literature, and its increase explained by the change of experimental conditions [22–25].

The results presented indicate that the Yoon–Nelson equation can be used for predicting of breakthrough curves

for lead ion removal by a fixed bed of clinoptilolite for different flow rates, or possibly for different bed depths that could provide a framework for scaling up the process.

Furthermore, we have found out how the change of one experimental condition, such as bed depth (H), affects the position and shape of the modelled breakthrough curve using evaluated parameters K_{YN} and τ. For this purpose, it is necessary to plot the dependence of K_{YN} and τ versus empty bed contact time (EBCT) based on results in Table 3 (Fig. 7).

For scaling up of the bed depth from 4 cm to 11.5 cm, at a constant flow rate of 3 ml/min, EBCT increases according to Eq. (7) and equals 4.33 min. These values are inserted into the x-axis on Fig. 7, and the values of K_{YN} and τ are evaluated. Their insertion into Eq. (13) for randomly chosen values of t and known initial concentrations
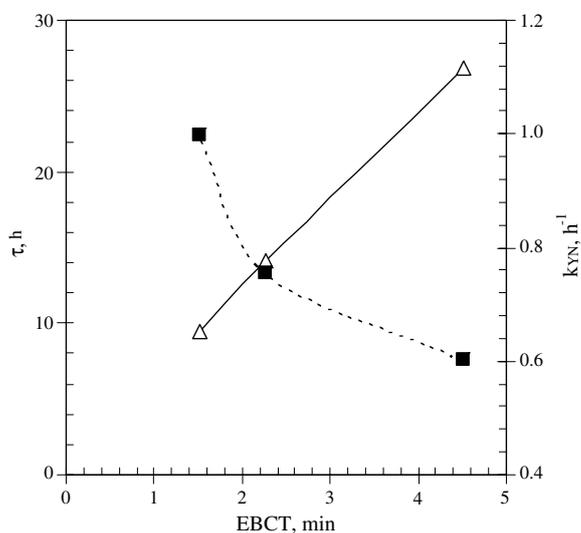

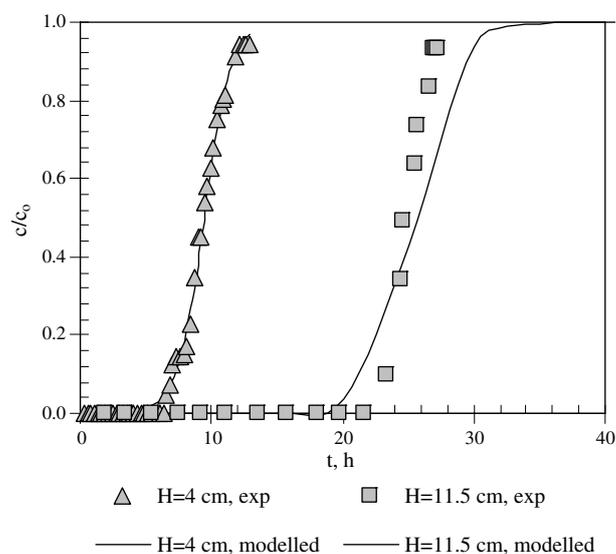Fig. 7. Dependence of parameters of the Yoon–Nelson model on the empty bed contact time.

Fig. 8. Comparison of experimental (points) and modelled (lines) curves for scaling up of depth of fixed bed from $H = 4$ cm to $H = 11.5$ cm.

Table 4
Comparison of experimentally obtained and modelled parameters of breakthrough curves for different bed depths, $Q = 3$ ml/min, $c_o = 1.024$ mmol/l

Parameter	$H = 4$ cm	$H = 11.5$ cm
K_{YN}, h^{-1}	1.000	0.600
τ, h	9.40	25.50
t_B, modelled h	6.43	20.55
t_E, modelled, h	12.38	30.40
t_B exp., h	6.58	21.67
t_E exp., h	12.11	28.28

c_o, gives the modelled, i.e., predicted curves plotted in Fig. 8.

In order to provide a test of correctness of the predicted curve, a new experiment is performed at the same initial concentration of 1.024 mmol/l and a flow rate of 3 ml/min, but at increased bed depth of 11.5 cm, using the same experimental procedure described in Section 2. The new experimental curve is also plotted and compared with its own previously predicted curve in Fig. 8. The comparison of breakthrough and exhaustion times for the experimental and modelled curves is shown in Table 4.

Their fit is satisfactory, it is better in the region of $c/c_o = 0.5$, and a deviation of the predicted curve from the experimental one for $H = 11.5$ cm is observed near the breakthrough and exhaustion points.

4. Conclusions

The column performance with a fixed bed of natural zeolite can be used for removal of lead ions from aqueous solutions. The achieved capacity of ion exchange for lead ions is in the range of results attained by authors that have examined similar systems. The capacities in the breakthrough and exhaustion points have relatively close values, which results in a sharp "S" shape of the curves due to the optimal choice of the ratio of particle/column diameters, and the ratio of bed depth/column diameter. The capacities C_B and C_E do not depend on the flow rate of the solution, in the flow range examined, which means that the same efficiency of the fixed bed can be reached in a significantly shorter time. The difference between C_B and C_E increases at increased flows, which negligibly decreases the column efficiency η. At higher values of flow rates, the height of the mass transfer zone h_Z increases and the empty bed contact time decreases. The Yoon and Nelson equation was applied to the experimental column data to investigate the dynamic behaviour of the fixed bed of clinoptilolite in the lead ion solution. The parameters of the model K_{YN} and τ have been calculated for each examined solution flow. The rate constant K_{YN} increases and the breakthrough time τ decreases with the increase of the lead solution flow. This is explained by increased mass transport through the film and faster saturation of the bed. The

parameters obtained from the fitting of experimental data to the model were used to generate modelled breakthrough curves. These calculated curves are in excellent agreement with the corresponding experimental curves. The parameters of the Yoon–Nelson model have been used for plotting of predicted breakthrough curves when scaling up the bed depth. The correctness of modelled curves was confirmed by a satisfying agreement with new experimental breakthrough curves.

Acknowledgments

References

[1] M. Vaca-Mier, R.L. Callejas, R. Gehr, B.E. Jimenez Cisneros, P.J.J. Alvarez, Water Res. 35 (2001) 373.
[2] F.A. Mumpton, in: C. Colella, F.A. Mumpton (Eds.), Natural zeolites: where have we been, where are we going? Natural zeolites for the third millennium, Napoli, 2000, p. 19.
[3] J. Perić, M. Trgo, N. Vukojević Medvidović, Water Res. 38 (2004) 1893.
[4] L. Ćurković, Š. Cerjan Stefanović, T. Filipan, Water Res. 31 (1997) 1379.
[5] M. Turan, U. Mart, B. Yuksel, M.S. Celik, Chemosphere 60 (2005) 1487.
[6] E. Maliou, M. Malamis, P.O. Sakellarides, Water Sci. Technol. 25 (1992) 133.
[7] V.J. Inglezakis, H. Grigoropoulou, J. Hazard. Mater. B 112 (2004) 37.
[8] L.D. Benefield, J.F. Judkins, B.L. Weand, Process chemistry for water and wastewater treatment, Prentice-Hall, Inc., New Jersey, 1982, pp. 377–390.
[9] V.K. Gupta, S.K. Srivastava, D. Mohan, Ind. Eng. Chem. Res. 36 (1997) 2207.
[10] N. Vukojević Medvidović, J. Perić, M. Trgo, Sep. Purif. Technol. 49 (2006) 237.
[11] V.J. Inglezakis, H.P. Grigoropoulou, Micropor. Mesopor. Mater. 61 (2003) 273.
[12] I. Voinovitch, J. Debrad-Guedon, J. Louvrier, The Analysis of Silicates, Israel Program for Scientific Translations, Jerusalem, 1966, pp. 127–129.
[13] E. Merck (Ed.), Complexometric Assay Methods with Triplex, Darmstadt, 1982, p. 55.
[14] A.S. Michaels, Ind. Eng. Chem. 44 (1952) 922.
[15] M. Panayotova, B. Velikov, J. Environ. Sci. Health A 37 (2002) 139.
[16] C. Colella, in: P. Misaelides, F. Macašek, T.J. Pinnavaia, C. Colella (Eds.), Natural Materials in Environmental Technology, Kluwer Academic Publishers., Dordrecht, 1999, p. 207.
[17] Z. Aksu, F. Gonen, Process. Biochem. 39 (2004) 599.
[18] Y. Sag, Y. Aktay, Process. Biochem. 36 (2001) 1187.
[19] Y.H. Yoon, J.H. Nelson, Am. Ind. Hyg. Assoc. J. 45 (1984) 509.
[20] R.S. Juang, S.H. Lin, T.Y. Wang, Chemosphere 53 (2003) 1221.
[21] S.H. Lin, C.Y. Huang, J. Environ. Eng. 126 (2000) 802.
[22] Z. Aksu, F. Gonen, Sep. Purif. Technol. 49 (2006) 205.
[23] O. Hamdaoui, J. Hazard. Mater. B 138 (2006) 293.
[24] R.S. Juang, H.C. Kao, W. Chen, Sep. Purif. Technol. 49 (2006) 36.
[25] E. Malkoc, Y. Nuhoglu, Y. Abali, Chem. Eng. J. 119 (2006) 61.